m^{6}A RNA methylation regulators contribute to malignant progression and have clinical prognostic impact in gliomas

Rui-Chao Chai[*,1,3,5], **Fan Wu**[*,1,5]**, Qi-Xue Wang**[*,4,5]**, Shu Zhang**[4]**, Ke-Nan Zhang**[1,5]**, Yu-Qing Liu**[1,5]**, Zheng Zhao**[1,5]**, Tao Jiang**[1,2,3,5]**, Yong-Zhi Wang**[1,2,3,5]**, Chun-Sheng Kang**[4,5,6]

[1]Department of Molecular Neuropathology, Beijing Neurosurgical Institute, Beijing Tiantan Hospital, Capital Medical University, Beijing 100160, China
[2]Department of Neurosurgery, Beijing Tiantan Hospital, Capital Medical University, Beijing 100160, China
[3]China National Clinical Research Center for Neurological Diseases, Beijing, China
[4]Laboratory of Neuro-Oncology, Tianjin Neurological Institute, Department of Neurosurgery, Tianjin Medical University General Hospital and Key Laboratory of Neurotrauma, Variation, and Regeneration, Ministry of Education and Tianjin Municipal Government, Tianjin 300052, China
[5]Chinese Glioma Genome Atlas Network (CGGA)
[6]Affiliated Cancer Hospital & Institute of Guangzhou Medical University, Guangzhou 510095, China
[*]Equal contribution

ABSTRACT

N6-methyladenosine (m^{6}A) RNA methylation, associated with cancer initiation and progression, is dynamically regulated by the m^{6}A RNA methylation regulators ("writers", "erasers" and "readers"). Here, we demonstrate that most of the thirteen main m^{6}A RNA methylation regulators are differentially expressed among gliomas stratified by different clinicopathological features in 904 gliomas. We identified two subgroups of gliomas (RM1/2) by applying consensus clustering to m^{6}A RNA methylation regulators. Compared with the RM1 subgroup, the RM2 subgroup correlates with a poorer prognosis, higher WHO grade, and lower frequency of *IDH* mutation. Moreover, the hallmarks of epithelial-mesenchymal transition and TNFα signaling via NF-κB are also significantly enriched in the RM2 subgroup. This finding indicates that m^{6}A RNA methylation regulators are closely associated with glioma malignancy. Based on this finding, we derived a risk signature, using seven m^{6}A RNA methylation regulators, that is not only an independent prognostic marker but can also predict the clinicopathological features of gliomas. Moreover, m^{6}A regulators are associated with the mesenchymal subtype and TMZ sensitivity in GBM. In conclusion, m^{6}A RNA methylation regulators are crucial participants in the malignant progression of gliomas and are potentially useful for prognostic stratification and treatment strategy development.

INTRODUCTION

In the traditional concept, epigenetics only involves the reversible chemical modification of DNA or proteins (histones) and regulates gene expression independent of DNA sequences, which could be heritable through cell division [1]. RNA modification was first discovered in the 1970s, but it has only recently been considered a third layer of epigenetics, along with the emerging functions of regulating RNA processing and metabolism

[1-7]. Currently, RNA modification has been identified in almost all forms of native cellular RNA, including mRNAs, tRNAs, rRNAs, small nuclear RNAs, small nucleolar RNAs, long noncoding RNAs (lncRNAs) and micro-RNAs (miRNA) [5-12]. It has been reported in several forms, including N1-methyladenosine, N7-methyladenosine, 5-methylcytosine, pseudouridine, N6,2'-O-dimethyladenosine (m6A) and 2'-O-methylation [5, 11, 13]. Among these, the m6A modification was the first identified and is the most abundant form of mRNA methylation in eukaryotes [11, 14, 15].

RNA modification, similar to DNA and protein modification, is dynamically regulated by methyl-transferases ('writers'), binding proteins ('readers'), and demethylases ('erasers') [6]. The prominent m6A methylation regulators consist of 'writers' such as methyltransferase like 3 (METTL3), METTL14, WT1-associated protein (WTAP), KIAA1429, RNA binding motif protein 15 (RBM15) and zinc finger CCCH domain-containing protein 13 (ZC3H13), 'readers' such as YTH domain-containing 1 (YTHDC1), YTH domain-containing 1 (YTHDC2), YTH N6-methyl-adenosine RNA binding protein 1 (YTHDF1), YTH N6-methyladenosine RNA binding protein 2 (YTHDF2) and heterogeneous nuclear ribonucleoprotein C (HNRNPC), and 'erasers' such as fat mass- and obesity-associated protein (FTO) and α-ketoglutarate-dependent dioxygenase alkB homolog 5 (ALKBH5) [6, 16-21]. The discovery of m6A RNA methylation regulators has dramatically increased our understanding of the function and mechanism of m6A modification in the posttranscriptional regulation of gene expression [6, 12, 15, 22, 23].

m6A modification not only plays a vital role in oocyte and central nervous system development [9, 16] but also has various regulatory functions in tumor initiation, progression and radio-resistance [4, 22, 24, 25]. Moreover, increasing evidence indicates that genetic changes and dysregulated expression of m6A RNA methylation regulators are closely associated with malignant progression in various kinds of cancer [4, 15, 21, 22, 26, 27]. Recently, an important study revealed that FTO expression is upregulated in *IDH*-mutant leukemia and plays an anti-tumor role through the FTO/m6A/MYC/CEBPA signaling pathway [28]. *IDH* mutation is also a major driver of mutation in glioma, and gliomas with *IDH* mutation have a better prognosis than *IDH* wildtype gliomas. The m6A RNA methylation regulators were also reported to play pivotal roles in glioma stem-like cell maintenance and radio-resistance [25, 26]. However, the literature lacks a comprehensive analysis of the expression of m6A RNA methylation regulators in gliomas with different clinicopathological

characteristics, their function in glioma malignant progression, and their prognostic value.

In this study, we systematically analyzed the expression of thirteen widely reported m6A RNA regulators in 904 gliomas with RNA sequencing data from the Chinese Glioma Genome Atlas (CGGA) (n = 309) and The Cancer Genome Atlas (TCGA) (n = 595) datasets. We provided the expression data of each m6A modification regulator with regard to different clinicopathological features. We found that the expression of m6A RNA methylation regulators plays important roles in the malignant progression of gliomas, and a signature with seven selected m6A RNA methylation regulators was designed to stratify the prognosis of gliomas.

RESULTS

Expression of m6A RNA methylation regulators is correlated with clinicopathological features in gliomas

Considering the important biological functions of each m6A RNA methylation regulator in tumorigenesis and development, we systematically investigated the relationships between each individual m6A RNA methylation regulator and the pathological features of gliomas, including WHO grade, *IDH* status, and 1p/19q codeletion status. The expression level of each m6A RNA methylation regulator and WHO grades are presented as heatmaps (Fig. 1A and B), showing that the expressions of most m6A RNA methylation regulators are significantly associated with WHO grades. The significant correlations between WHO grades and expression levels of WTAP, RBM15, YTHDF, ALBKH5, and FTO were also confirmed by quantitative analyses in both the CGGA (Fig. 1C) and TCGA datasets (Fig. 1D). As the WHO grade increased, the expression of WTAP, RBM15, YTHDF and ALBKH5 increased, while the expression of FTO decreased.

We then studied the relationship between *IDH* status and expression levels of each m6A RNA methylation regulator in lower-grade gliomas (LGG, Fig. 1E and 1F) and glioblastomas (GBM, Fig. 1G), respectively. The results showed that expression levels of ALKBH5, YTHDF2, RBM15, METTL3, METTL14, FTO and YTHDC1 are significantly different between LGG with mutant-*IDH* and LGG with wildtype-*IDH* in both CGGA (Fig. 1E) and TCGA (Fig. 1F) datasets. FTO, YTHDC1 and METTL3 were also differentially expressed between GBM with and without *IDH* mutation in the CGGA dataset (Fig. 1G). However, we were unable to compare the expression of m6A RNA methylation regulators between GBM with and without
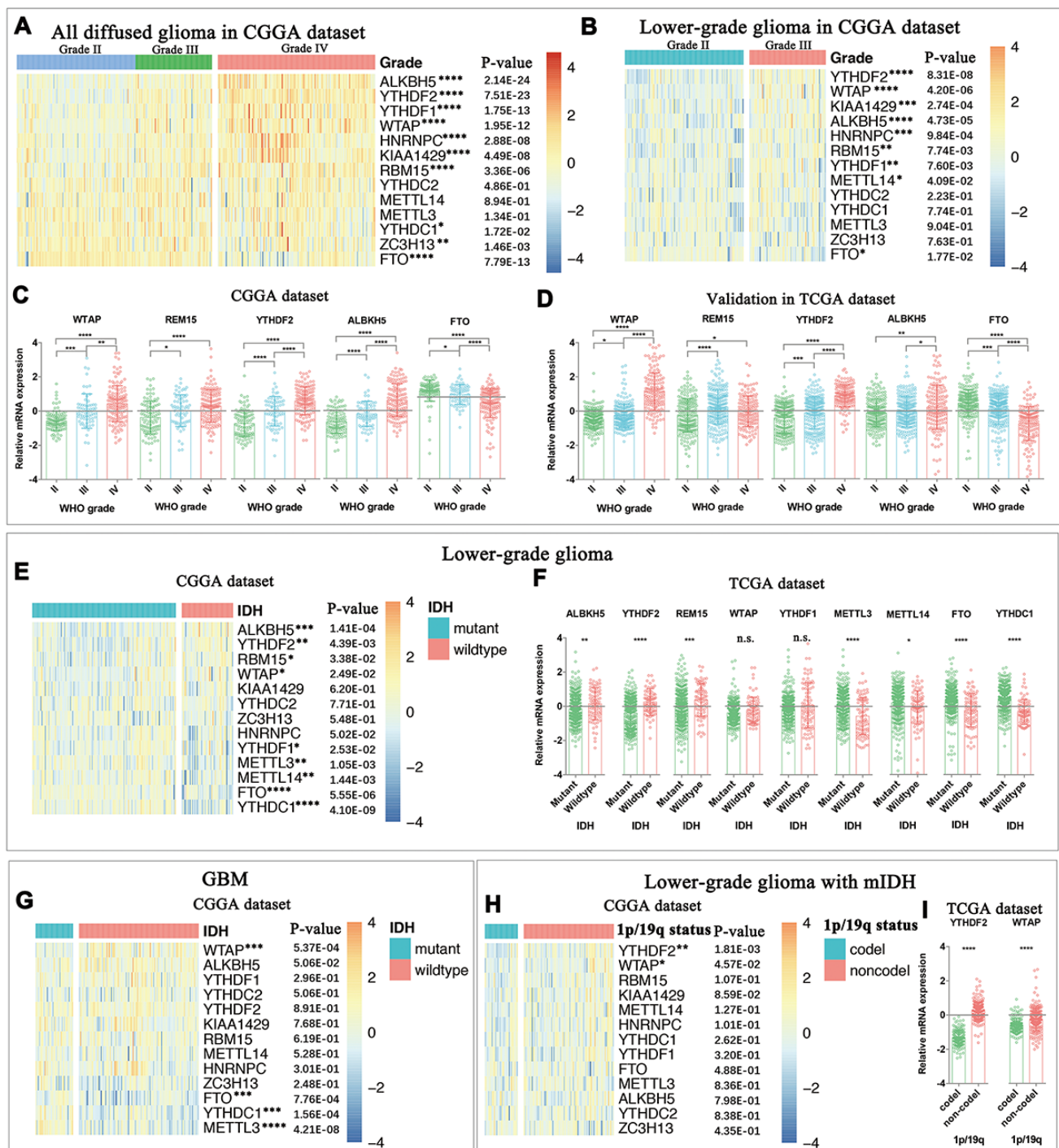
Figure 1. Expression of m⁶A RNA methylation regulators in gliomas with different clinicopathological features. (**A-D**) The expression levels of thirteen m⁶A RNA methylation regulators in gliomas with different WHO grades. (**E-F**) The expression levels of m⁶A RNA methylation regulators in LGG with different *IDH* status. (**G**) The expression levels of m⁶A RNA methylation regulators in GBM with different *IDH* status. (**H**) The expression levels of m⁶A RNA methylation regulators in *IDH*-mutant (m*IDH*) LGG with different 1p/19q codeletion status. * P < 0.05, ** P < 0.01, *** P < 0.001 and **** P < 0.0001.

IDH mutation in the TCGA dataset because of the dramatically imbalanced numbers of *IDH*-mutant GBM (n=10) and *IDH*-wildtype GBM (139). In the LGG with mutant-*IDH*, we observed that the expressions of YTHDF2 and WTAP were highly correlated with the status of 1p/19q codeletion (1p/19q codel).

We noticed that the expression of both METTL3 and METTL14 were not correlated with the WHO grade of gliomas. Considering METTL16 is also a putative m6A methyltransferase and knockdown of METTL16 could result in approximately 20% decrease of m6A [29], we also investigated the expression of METTL16 in gliomas with different malignancy status in the CGGA dataset (Figure S1). METTL16 expression was also not correlated with the WHO grade of gliomas. Though METTL16 expression correlated to the *IDH* status in LGG (P<0.001) and GBM (P<0.05), it did not have prognostic value in any pathological subgroup of gliomas (data not shown). In addition, the expression information was also not included in the TCGA dataset, so METTL16 was not included in the following section of this study.

Moreover, we also observed that the genetic change (mutation or coy number change) frequencies of the thirteen m6A RNA methylation regulators were very low (all ≤ 1.1%) in gliomas (Figure S2), indicating that

the expression changes of these m6A RNA methylation regulators were not caused by the genetic changes of the corresponding genes.

Consensus clustering of m6A RNA methylation regulators identified two clusters of gliomas with distinct clinical outcomes and clinicopathological features

Based on the expression similarity of m6A RNA methylation regulators, k = 3 seemed to be an adequate selection with clustering stability increasing from k = 2 to 10 in the CGGA datasets (Fig. 2A and B). However, we noticed that 293 out of 309 gliomas clustered into one of the two subgroups in the CGGA dataset (Fig. 2C and Figure S3). Thus, we compared the clinicopathological features of these two subgroups clustered by k=2, namely, RM1 and RM2 (Fig. 2C) datasets. The RM1 subgroup is significantly correlated with younger age at diagnosis (P < 0.0001), lower grade (P < 0.0001), proneural or neural subtypes (P < 0.0001), *IDH-*
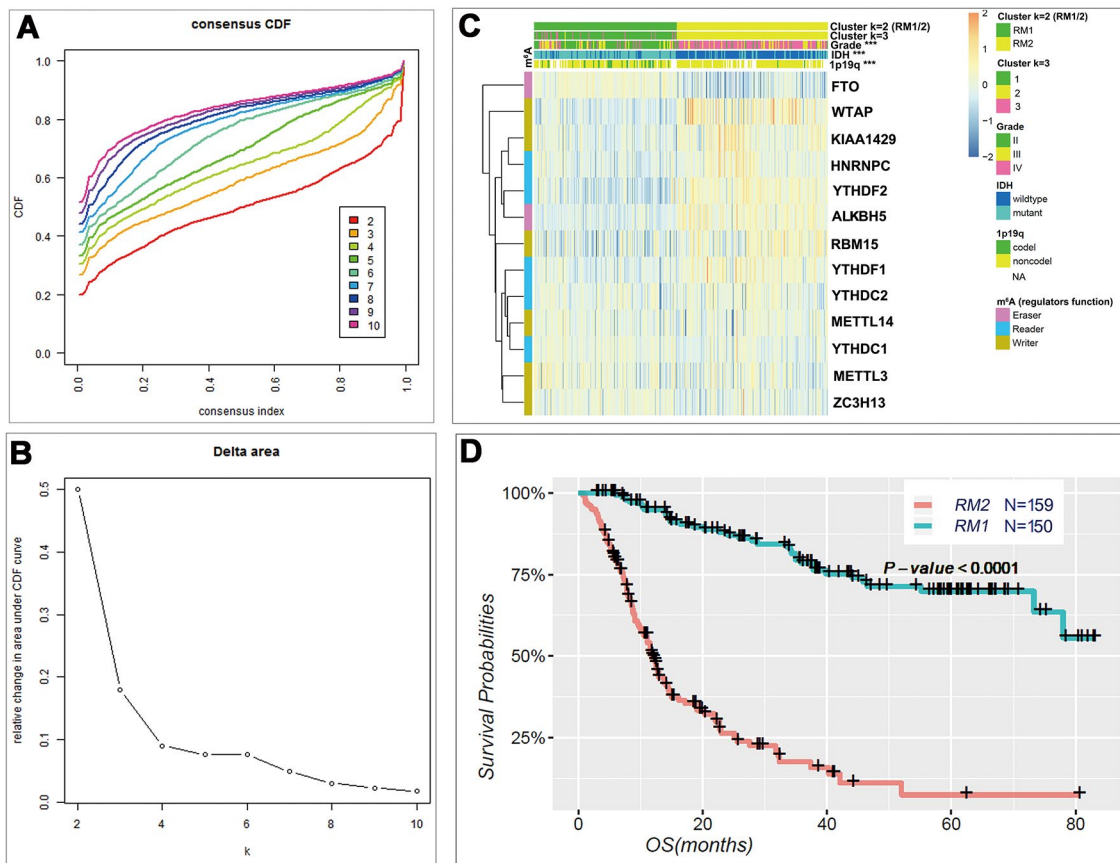

Figure 2. Differential clinicopathological features and overall survival of gliomas in the RM1/2 subgroups. (**A**) Consensus clustering cumulative distribution function (CDF) for k = 2 to 10. (**B**) Relative change in area under CDF curve for k = 2 to 10. (**C**) Heatmap and clinicopathologic features of the two clusters (RM1/2) defined by the m6A RNA methylation regulators consensus expression. (**D**) Kaplan–Meier overall survival (OS) curves for 309 CGGA glioma patients.

mutational status (P < 0.0001) and 1p/19q codel status (P < 0.0001). The RM2 subgroup mainly contains gliomas with an older age at diagnosis, glioblastoma (GBM) phenotype, classic or mesenchymal subtypes, *IDH*-wildtype status and 1p/19q noncodel status (Table S2). Moreover, we observed a significantly shorter overall survival (OS) in the RM2 subgroup than the RM1 subgroup (Fig. 2D).

Categories identified by consensus clustering are closely correlated to the malignancy of gliomas

The above findings suggested that the clustering result was closely correlated to the malignancy of the gliomas. To better understand the interactions among the thirteen m⁶A RNA methylation regulators, we also analyzed the interaction (Fig. 3A) and correlation (Fig. 3B) among
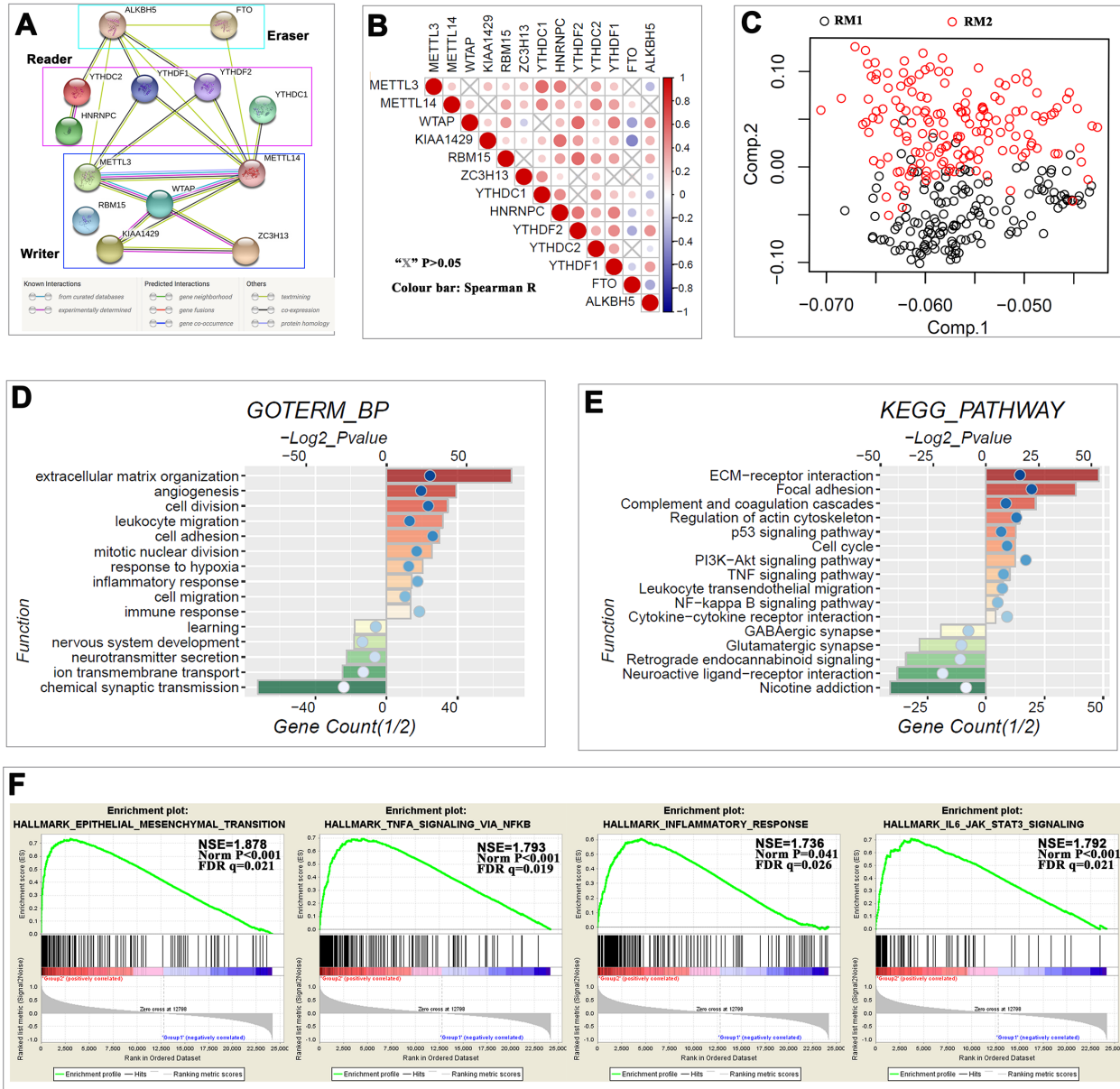

Figure 3. Interaction among m⁶A RNA methylation regulators and functional annotation of gliomas in RM1/2 subgroups. (**A**) The m⁶A modification-related interactions among the 13 m⁶A RNA methylation regulators. (**B**) Spearman correlation analysis of the 13 m⁶A modification regulators. (**C**) Principal component analysis of the total RNA expression profile in the CGGA dataset. Gliomas in the RM2 subgroup are marked with red. (**D–E**) Functional annotation of the genes with higher expression in the RM2 subgroup (red bar chart) or RM1 subgroup (green bar chart) using GO terms of biological processes (**D**) and KEGG pathway (**E**). (**F**) GSEA revealed that genes with higher expression in RM2 subgroup were enriched for hallmarks of malignant tumors.

these regulators. WTAP seems to be the hub gene of the 'writers', and its interactions or coexpressions with METTL3, METTL14, KIAA1429 and ZC3H13 are supported both by experimental data and by text mining in the String database (Fig. 3A). The expression of WTAP was also significantly correlated with the 'writers' of METTL14, KIAA1429 and RBM15 in gliomas (Fig. 3B). There are several independent interaction groups in 'readers', suggesting the diverse functions of different 'readers' (Fig. 3A), but the expressions of YTHDF2, YTHDC2 and YTHDF1 were significantly correlated with each other in gliomas (Fig. 3B). Only text mining evidence supported the interaction of ALKBH5 and FTO in the String database (Fig. 3A), and the expressions of ALKBH5 and FTO were negatively correlated with each other in gliomas (Fig. 3B). Moreover, the expressions of WTAP, RBM15, YTHDF2, YTHDF1 and ALKBH5 were highly correlated with each other, and all of their expressions were negatively correlated with FTO in gliomas (Fig. 3B). These findings were consistent with

that the expression levels of WTAP, RBM15, YTHDF2, YTHDF1 and ALKBH5 being positively correlated with the increasing malignancy of gliomas, while the expression levels of FTO are negatively correlated with the increasing malignancy of gliomas (Figs. 1 and 2).

We further used principal component analysis (PCA) to compare the transcriptional profile between RM1 and RM2 subgroups. The results showed a clear distinction between them (Fig. 3C). We identified genes that were significantly upregulated (Score(d) for SAM > 8, fold change >2, and normalized P < 0.01) or downregulated (Score(d) for SAM < -8, fold change < 0.5, and normalized P < 0.01) in the RM2 subgroup, and then annotated their function using gene ontology (GO) pathway analysis for biological processes (Fig. 3D). The results indicated that upregulated genes are enriched in malignancy-related biological processes, including cell proliferation, extracellular matrix organization, angiogenesis, migration, and immune response, among others. Similar changes in
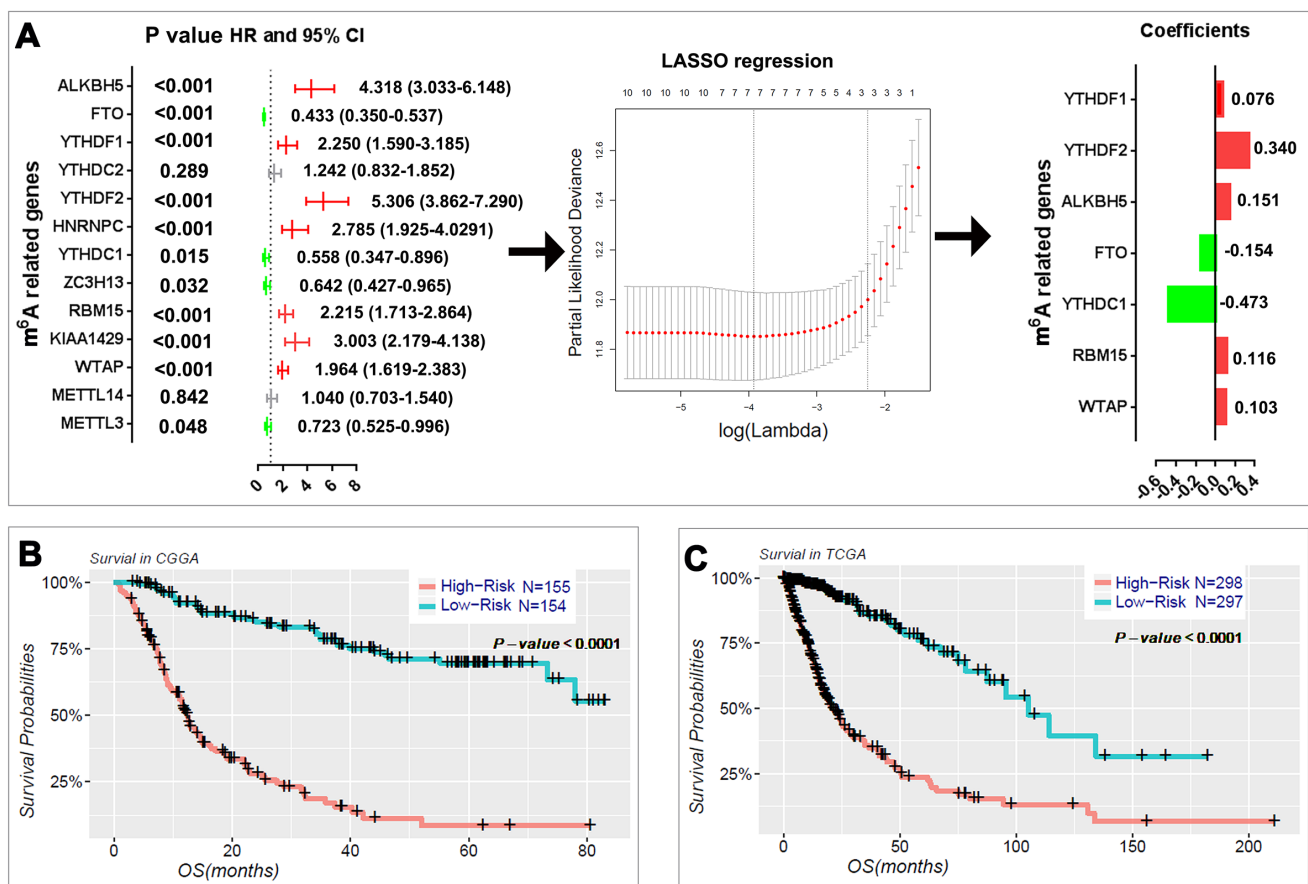
Figure 4. Risk signature with seven m⁶A RNA methylation regulators. (A) The process of building the signature containing seven m⁶A RNA methylation regulators. The hazard ratios (HR), 95% confidence intervals (CI) calculated by univariate Cox regression and the coefficients calculated by multivariate Cox regression using LASSO are shown. (B–C) Kaplan–Meier overall survival (OS) curves for patients in the CGGA (B) and TCGA (C) datasets assigned to high- and low-risk groups based on the risk score.

corresponding signaling pathways were also observed in the Kyoto Encyclopedia of Genes and Genomes (KEGG) pathway analysis (Fig. 3E). Furthermore, gene set enrichment analysis (GSEA) revealed that the malignant hallmarks of tumors, including epithelial-mesenchymal transition (NES=1.88, normalized P < 0.001), TNFα signaling via NF-κB (NES=1.79, normalized P < 0.001), inflammatory response (NES=1.74, normalized P = 0.041) and IL6/JAK/STAT3 signaling (NES=1.79, normalized P < 0.001), were significantly associated with the RM2 subgroup (Fig. 3F). All of these findings indicated that the two categories identified by consensus clustering are closely correlated with the malignancy of gliomas.

Prognostic value of m^{6}A RNA methylation regulators, and a risk signature built using seven selected m^{6}A RNA methylation regulators

We next sought to investigate the prognostic role of m^{6}A RNA methylation regulators in gliomas. We performed a univariate Cox regression analysis on the expression levels in the CGGA dataset (Fig. 4A). The results indicated that eleven out of thirteen tested genes are significantly correlated with OS (P < 0.05). Among these eleven genes, ALKBH5, YTHDF1, YTHDF2, HNRNPC, RBM15, KIAA1429, and WTAP are risky genes with HR > 1, while FTO, YTHDC1, ZC3H13, and METTL3 are protective genes with HR < 1. We also investigated the prognostic value for each m^{6}A RNA methylation regulator in stratified LGG (Table S3) and GBM (Table S4). For the genes with prognostic value in LGG, the expression levels of YTHDF2, WTAP, ALKBH5, RBM15, KIAA1429, HNRNPC, YTHDF1, and FTO are significantly correlated with the overall survival (OS) of patients with *IDH*-mutant and 1p/19q noncodel LGG. Among these genes, YTHDF2, KIAA1429, HNRNPC, and YTHDF1 also have prognostic value in *IDH*-wildtype LGG. In the GBM, the expressions of FTO, YTHDF2, and RBM15 have prognostic value in *IDH*-wildtype GBM; and FTO also has prognostic value in *IDH*-mutant GBM.

To better predict the clinical outcomes of gliomas with m6A RNA methylation regulators, we applied the least absolute shrinkage and selection operator (LASSO) Cox regression algorithm to the eleven prognosis-associated genes in the CGGA dataset, which we used as a training set (Fig. 4A). Seven genes were selected to build the risk signature based on the minimum criteria, and the coefficients obtained from the LASSO algorithm were used to calculate the risk score for both the training dataset (CGGA) and the validation dataset (TCGA). To investigate the prognostic role of the seven-gene risk signature, we separated the glioma patients in the CGGA (n = 309) and TCGA (n = 595) datasets into low-

and high-risk groups based on the median risk score and observed significant differences in OS between the two categories (both P < 0.0001; Fig. 4B, C).

Prognostic risk scores showed strong associations with clinicopathological features in gliomas

The heatmap shows the expression of the seven selected m^{6}A RNA methylation regulators in high- and low-risk patients in the CGGA dataset (Fig. 5A). We observed significant differences between the high- and low-risk groups with respect to WHO grade (P < 0.001), age (P < 0.001), *IDH* status (P < 0.001), 1p/19q codel status (P < 0.001), TCGA subtypes (P < 0.001), and RM1/2 subgroups (P < 0.001). We also examined the association between the risk scores and each clinicopathological feature. We observed that risk scores are significantly different between patients stratified by WHO grade, TCGA subtype, age, *IDH* status, 1p/19q codel status, and RM1/2 subgroups, but not by gender, in both the CGGA (Fig. 5B–H) and TCGA datasets (Figure S4). The ROC curve shows that the risk score can perfectly predict three-year survival rates for glioma patients (AUC = 90.3%), RM1/2 subgroups (AUC = 98.6%), glioma *IDH*-mutant status (AUC = 86.3%) and glioma 1p/19q codel status (AUC = 82.3%). Furthermore, the predictive efficiency is better than that of the WHO grade and age (Fig. 5I-L). These results indicate that the risk scores calculated with the signature can accurately predict glioma patient outcomes and clinicopathological features, especially for the RM1/2 subgroups.

We then performed univariate and multivariate Cox regression analyses for the CGGA dataset to determine whether the risk signature is an independent prognostic indicator. By univariate analysis, the risk score, 1p/19q codel status, *IDH* status, age and WHO grade were all correlated with the OS. When including these factors into the multivariate Cox regression, the risk score and WHO grade remained significantly associated with the OS (both P < 0.001, Fig. 5M). Similar results were found in the validation of the TCGA dataset; the risk score (P = 0.027), *IDH* status (P < 0.001), age (P < 0.001) and WHO grade (P = 0.005) remained significantly associated with the OS in the multivariate regression (Fig. 5N). These results confirmed that the risk score derived from m^{6}A RNA methylation regulators can independently predict prognosis in glioma patients.

We also determined the prognostic value of the risk signature for different WHO grades. We found that patients with high risk scores had significantly shorter OS than those with low scores in WHO grade II and III gliomas (Fig. 6A, B) and GBM (Fig. 6C). Meanwhile,
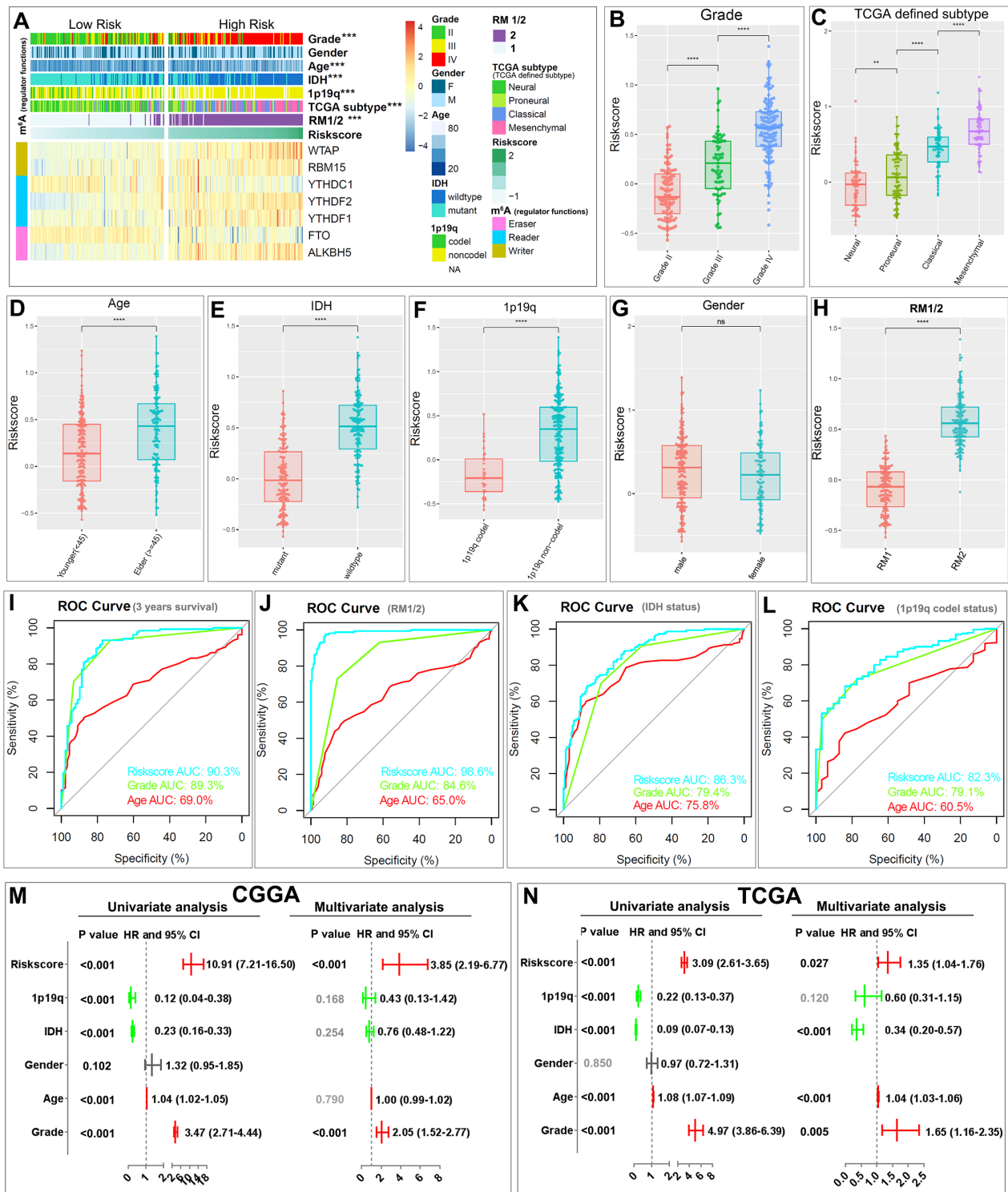
Figure 5. Relationship between the risk score, clinicopathological features and RM1/2 subgroups. (**A**) The heatmap shows the expression levels of the seven m⁶A RNA methylation regulators in low- and high-risk gliomas. The distribution of clinicopathological features was compared between the low- and high-risk groups. *** P<0.001 (**B–H**) Distribution of risk scores in the CGGA dataset stratified by WHO grade (**B**), TCGA subtype (**C**) age (**D**), *IDH* status (**E**), 1p/19q codel status (**F**), gender (**G**) and RM1/2 subgroups (**H**). **P < 0.01, and ****P < 0.0001. (**I-L**) ROC curves showed the predictive efficiency of the risk signature, WHO grade, and age on the three-year survival rate (**I**), RM1/2 subgroups (**J**), *IDH*-mutant status (**K**) and 1p/19q codel status (**L**). (**M-N**) Univariate and multivariate Cox regression analyses of the association between clinicopathological factors (including the risk score) and overall survival of patients in the CGGA (**M**) and TCGA (**N**) datasets. ns no significance, *** P < 0.001 and **** P < 0.0001.
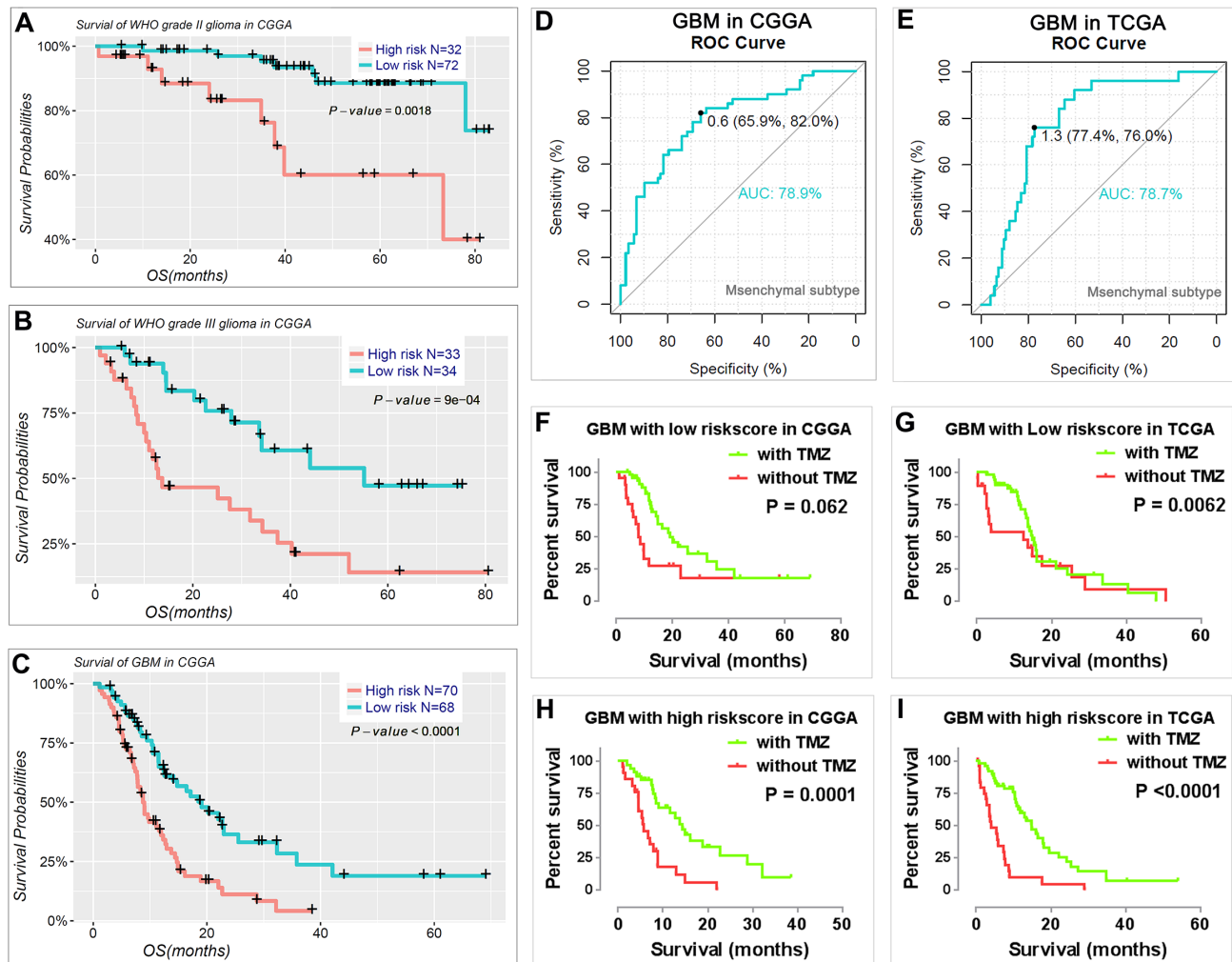
Figure 6. Prognostic value of the risk signature in patients stratified by WHO grade. (**A–C**) Kaplan–Meier overall survival curves for patients with WHO grade II (**A**), WHO grade III (**B**), and GBM (**C**). (**D-E**) ROC curves showed the predictive efficiency of the risk signature on mesenchymal subtype in GBM of CGGA (**D**) and TCGA (**E**) datasets. (**F-I**) GBM patients with high risk scores had a greater benefit from TMZ chemotherapy.

we also observed that the risk score had prognostic value in gliomas stratified by the integrated diagnosis of WHO grade 2016 (Figure S5). Moreover, the risk score could also predict the mesenchymal subtype in GBM for both CGGA (Fig. 6D) and TCGA datasets (Fig. 6E). Consistent with this finding, the patients with a high-risk score were also more sensitive to TMZ treatment in GBM for both CGGA and TCGA datasets (Fig. 6F-I).

DISCUSSION

Malignant progression and high recurrence rate render gliomas the most lethal type of primary brain tumor [30-32]. Traditional epigenetics, limited to DNA or protein modification, has a variety of functions in

glioma initiation, malignant progression, and prognosis [33-35]. In this study, we demonstrated that the expression of regulators of another area of epigenetics—RNA m^6A RNA methylation—is also closely associated with the malignancy and prognosis of gliomas. We identified two glioma subgroups, RM1/2, by consensus clustering based on the expression of m^6A RNA methylation regulators. The RM1/2 subgroups not only influenced the prognosis and clinicopathological features but were also closely correlated with biological processes, key signaling pathways, and hallmarks of malignant gliomas. In addition, we also derived a prognostic risk signature with seven selected m^6A RNA methylation regulators, which stratified the OS of patients with gliomas into high- and low-risk categories.

Among the m6A RNA methylation regulators, the writers METTL3 and METTL14 were reported as suppressor genes in GBM but oncogenes in acute myelocytic leukemia (AML) and hepatocellular carcinoma [15, 26]; the reader YTHDF2 promotes cancer cell proliferation in pancreatic cancer [36]; the eraser ALKBH5 functions as an oncogene in both GBM and breast cancer [4, 37]; and the eraser FTO is an oncogene in AML and glioma [4, 28]. These findings suggested that up- or downregulation of specific RNA m6A methylation regulators are linked to mis-regulated RNAs in tumors, and the same m6A methylation regulators may have distinct functions in different tumors.

In this section, we comprehensively analyzed the expression of all m6A RNA methylation regulators in gliomas with different clinicopathological features. As an m6A methylation writer, the expression of METLL3 was decreased in the mesenchymal subtype or *IDH*-wildtype gliomas. WTAP expression was significantly increased in high-grade, mesenchymal subtype, *IDH*-wildtype, 1p/19q noncodel and elderly glioma patients, indicating potential functions of WTAP in glioma malignancy. For the m6A methylation readers, the expression of HNRNPC, YTHDF1, and YTHDF2 was

significantly increased in high-grade gliomas. Furthermore, the expression of YTHDF2 is highly correlated with 1p/19q codeletion (1p/19q codel) status. For m6A methylation erasers, although both ALKBH5 and FTO were reported as oncogenes in GBM [4], their expression varies dramatically across different clinico-pathological features. Interestingly, the expression of FTO was significantly deceased in gliomas with malignant clinicopathological features, such as higher WHO grade, mesenchymal subtype, *IDH*-wildtype status, 1p/19q noncodel and older ages at diagnosis. Unlike ALKBH5, FTO could mediate the demethylation of both internal m6A and N6, 2-O-dimethyladenosine (m6Am) at the +1 position from the 5' cap in mRNA [38]. Recently, FTO was found to preferentially mediate the demethylation of m6Am rather than of m6A [39]. This also indicates that FTO and ALKBH5 may preferentially mediate demethylation of different methylation targets in glioma, and it is worth investigating in future studies. Taken together, the expression of m6A RNA methylation regulators is closely associated with malignant clinicopathological features in gliomas. Moreover, these findings are also useful for developing novel therapeutic methods through characterizing the expression of each individual m6A methylation
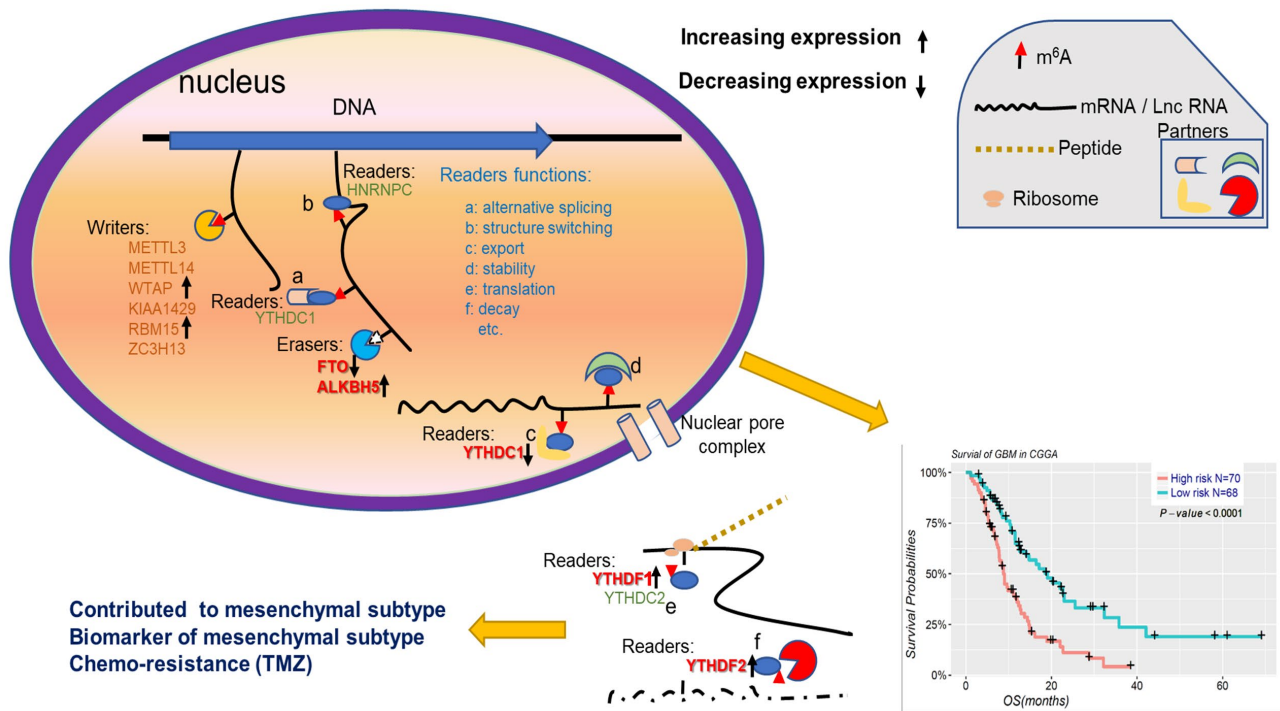

Figure 7. Summary for the expression changes and potential functions of m6A RNA methylation regulators in gliomas.

regulator in gliomas, as chemicals targeting m⁶A methylation are considered a new method for cancer therapy [22, 40].

This study uncovered that the m⁶A RNA methylation regulators were also correlated with the biological processes and signaling pathways of glioma malignant progression. The role of RNA m⁶A methylation in cancer has only been ascertained in recent years. Several biological processes and signaling pathways that it affects have been identified, including tumor stem cell growth; self-renewal, and tumorigenesis [4, 26]; RNA metabolism, including mRNA/miRNA/ lncRNA biogenesis, processing and exporting [22]; DNA damage response secondary to radio- or chemotherapy [22, 41]; the IL-7/STAT5/SOCS pathways [42]; and the FTO/m⁶A/MYC/enhancer-binding protein alpha signaling pathway [28]. Here, we revealed that in glioma, the expression of m⁶A RNA methylation regulators is significantly associated with biological processes, such as extracellular matrix, angiogenesis, cell division, response to hypoxia, inflammatory response, immune response and others, as well as with signaling pathways, such as ECM-receptor interaction, p53, cell cycle, PI3K-Akt, TNF, NFκB and others.

Whether the expression level of m⁶A RNA methylation regulators can be used as a prognostic maker is an important topic of research [4]. In this study, our glioma prognostic signature derived using seven m⁶A RNA methylation regulators was found to be of value. In addition, we also determined the prognostic value of the signature for WHO grades II, III, and IV gliomas in both the CGGA and TCGA dataset. Moreover, the risk score also had prognostic value in gliomas stratified by WHO 2016 grades (Figure S5). As we observed, though the signature risk score can stratify the OS for *IDH*-mutant and 1p/19q noncodel lower grade gliomas, *IDH*-wildtype lower grade gliomas, and *IDH*-wildtype GBM in the CGGA dataset, it cannot distinguish the OS in the TCGA dataset (data not shown). A similar scenario was also observed in the multivariate COX analysis. This may be caused by the strong correlation between the risk signature and *IDH* status.

In conclusion, our findings systematically demonstrated the expression, potential function, and prognostic value of m⁶A RNA methylation regulators in gliomas (Figure 7). The expressions of m⁶A RNA methylation regulators, which are highly associated with the malignant clinicopathological features of gliomas, are also significantly correlated with the increased expression levels of genes enriched in the biological processes and signaling pathways that promote the malignant progression of gliomas. In summary, our

study provides important evidence for future examination of the role of RNA m⁶A methylation in gliomas.

MATERIALS AND METHODS

Datasets

The RNA-seq transcriptome data and corresponding clinicopathological information were obtained for 309 glioma patients from CGGA (www.cgga.org.cn) and 595 glioma patients from TCGA (http://cancergenome.nih.gov/). For the RNA-seq data, reads per kilobase of transcript per million mapped reads values were obtained for the CGGA samples [27], and values normalized by expectation-maximization were obtained for the TCGA samples. The study protocol was approved by the ethics committee of Beijing Tiantan Hospital. Clinicopathological information for the CGGA and TCGA datasets is summarized in Supplementary Table S1.

Selection of m⁶A RNA methylation regulators

We first collated a list of sixteen m⁶A RNA methylation regulators from published literature, [6, 15, 21] and then we restricted the list to genes with available RNA expression data in the CGGA and TCGA datasets. This yielded a total of thirteen m⁶A RNA methylation regulators. Then, we systematically compared the expression of these m⁶A RNA methylation regulators in gliomas with different clinicopathological features.

Bioinformatic analysis

To investigate the function of m⁶A RNA methylation regulators in gliomas, we clustered the gliomas into different groups with "ConsensusClusterPlus" (50 iterations, resample rate of 80%, and Pearson correlation, http://www.bioconductor.org/). We used PCA with the R package for R v3.4.1 to study the gene expression patterns in different glioma groups. GO and KEGG pathway enrichment analyses were performed with the Database for Annotation, Visualization, and Integrated Discovery (http://david.abcc.ncifcrf.gov/home.jsp) to functionally annotate genes that are differentially expressed in different groups. Interactions among m⁶A RNA methylation regulators were analyzed using the STRING database (http://www.string-db.org/). GSEA was performed to investigate the functions correlated with different subgroups of gliomas.

To determine the prognostic value of m⁶A RNA methylation regulators, we performed univariate Cox regression analyses of their expression in the CGGA

dataset. From this, we identified eleven genes significantly associated with survival ($P < 0.05$), which we selected for further functional analysis and development of a potential risk signature with the LASSO Cox regression algorithm [43-46]. Finally, seven genes and their coefficients were determined by the minimum criteria, selecting the best penalty parameter λ associated with the smallest 10-fold cross validation within the training set. The risk score for the signature was calculated using the formula:

$$\text{Risk score} = \sum_{i=1}^{n} \text{Coef}_i * x_i,$$

where Coef_i is the coefficient, and x_i is the z-score-transformed relative expression value of each selected gene. This formula was used to calculate a risk score for each patient in both the training (CGGA) and validation (TCGA) datasets.

Statistical analysis

One-way ANOVA was used to compare the expression level of m6A RNA methylation regulators in gliomas with different WHO grades and TCGA subtypes, and t-tests were used to compare the expression levels in gliomas for age, gender, *IDH* status, and 1p/19q codel status.

Patients were clustered into two groups by consensus expression of m6A RNA methylation regulators or were divided into high- and low-risk groups using the median risk score (derived from the risk signature) as the cutoff value. Chi-square tests were used to compare the distribution of gender, WHO grade, TCGA subtype, *IDH* status, and 1p/19q codeletion status between the two risk groups.

To compare the risk scores of the signature for gliomas with different clinicopathologies, a one-way ANOVA or t-test was performed to compare the risk scores in patients grouped by clinical or molecular-pathological characteristics. Univariate and multivariate Cox regression analyses were performed to determine the prognostic value of the risk score and various clinical and molecular-pathological characteristics.

The prediction efficiency of the risk signature, WHO grade and age for 3-year survival, RM1/2 groups, *IDH*-mutant status and 1p/19q codeletion status were tested with operating characteristic (ROC) curves.

The Kaplan–Meier method with a two-sided log-rank test was used to compare the OS of the patients in the RM1/2 groups or in the high- and low-risk groups. All statistical analyses were conducted using R v3.4.1 (https://www.r-project.org/), SPSS 16.0 (SPSS Inc., Chicago, IL) and Prism 7 (GraphPad Software Inc., La Jolla, CA).

Abbreviations

Long noncoding RNAs: lncRNAs; micro-RNA: miRNA; N6,2'-O-dimethyladenosine: (m6A); Methyl-transferase-Like 3: METTL3; Wilms Tumor 1-Associated Protein: WTAP); domain-containing protein 13: ZC3H13; obesity-associated protein: FTO; α-ketoglutarate-dependent dioxygenase alkB homolog 5: ALKBH5; the Chinese Glioma Genome Atlas: CGGA; The Cancer Genome Atlas: TCGA; 1p/19q codeletion: 1p/19q codel; glioblastoma: GBM; principal component analysis: PCA; Gene Ontology: GO; Kyoto Encyclopedia of Genes and Genomes: KEGG; Gene Set Enrichment Analysis: GSEA; the least absolute shrinkage and selection operator: LASSO; receiver operating characteristic: ROC; overall survival: OS; acute myelocytic leukemia: AML.

AUTHOR CONTRIBUTIONS

Rui-Chao Chai, Yong-Zhi Wang and Chun-Sheng Kang conceived and designed the study, Rui-Chao Chai, Fan Wu and Qi-Xue Wang crafted the literature search, figures and tables, and was responsible for the writing and critical reading of the manuscript. Shu Zhang and Ke-Nan Zhan Yu-Qing Liu and Zheng Zhao contributed to the data collection and analysis and the critical reading of manuscript. Tao Jiang, Yong-Zhi Wang and Chun-Sheng Kang supervised and contributed to the critical reading of manuscript.

CONFLICTS OF INTEREST

The authors declare that they have no competing interests.

REFERENCES

1. Fu Y, Dominissini D, Rechavi G, He C. Gene expression regulation mediated through reversible m6A RNA methylation. Nat Rev Genet. 2014; 15:293–306. https://doi.org/10.1038/nrg3724

2. He C. Grand challenge commentary: RNA epigenetics? Nat Chem Biol. 2010; 6:863–65. https://doi.org/10.1038/nchembio.482

3. Zhao BS, He C. Fate by RNA methylation: m6A steers stem cell pluripotency. Genome Biol. 2015; 16:43. https://doi.org/10.1186/s13059-015-0609-1

4. Pan Y, Ma P, Liu Y, Li W, Shu Y. Multiple functions of m6A RNA methylation in cancer. J Hematol Oncol. 2018; 11:48. https://doi.org/10.1186/s13045-018-0590-8

5. Roundtree IA, Evans ME, Pan T, He C. Dynamic RNA modifications in gene expression regulation. Cell. 2017; 169:1187–200. https://doi.org/10.1016/j.cell.2017.05.045

6. Yang Y, Hsu PJ, Chen YS, Yang YG. Dynamic transcriptomic m6A decoration: writers, erasers, readers and functions in RNA metabolism. Cell Res. 2018; 28:616–24. https://doi.org/10.1038/s41422-018-0040-8

7. Wang X, Lu Z, Gomez A, Hon GC, Yue Y, Han D, Fu Y, Parisien M, Dai Q, Jia G, Ren B, Pan T, He C. N6-methyladenosine-dependent regulation of messenger RNA stability. Nature. 2014; 505:117–20. https://doi.org/10.1038/nature12730

8. Bartosovic M, Molares HC, Gregorova P, Hrossova D, Kudla G, Vanacova S. N6-methyladenosine demethylase FTO targets pre-mRNAs and regulates alternative splicing and 3'-end processing. Nucleic Acids Res. 2017; 45:11356–70. https://doi.org/10.1093/nar/gkx778

9. Yang D, Qiao J, Wang G, Lan Y, Li G, Guo X, Xi J, Ye D, Zhu S, Chen W, Jia W, Leng Y, Wan X, Kang J. N6-Methyladenosine modification of lincRNA 1281 is critically required for mESC differentiation potential. Nucleic Acids Res. 2018; 46:3906–20. https://doi.org/10.1093/nar/gky130

10. Leighton LJ, Bredy TW. Functional Interplay between Small Non-Coding RNAs and RNA Modification in the Brain. Noncoding RNA. 2018; 4:E15. https://doi.org/10.3390/ncrna4020015

11. Du K, Zhang L, Lee T, Sun T. m(6)A RNA methylation controls neural development and is involved in human diseases. Mol Neurobiol. 2018. https://doi.org/10.1007/s12035-018-1138-1

12. Liu F, Clark W, Luo G, Wang X, Fu Y, Wei J, Wang X, Hao Z, Dai Q, Zheng G, Ma H, Han D, Evans M, et al. ALKBH1-mediated tRNA demethylation regulates translation. Cell. 2016; 167:1897. https://doi.org/10.1016/j.cell.2016.11.045

13. Bohnsack MT, Sloan KE. Modifications in small nuclear RNAs and their roles in spliceosome assembly and function. Biol Chem. 2018; 399:1265–76. https://doi.org/10.1515/hsz-2018-0205

14. Liu N, Pan T. N6-methyladenosine–encoded epitranscriptomics. Nat Struct Mol Biol. 2016; 23:98–102. https://doi.org/10.1038/nsmb.3162

15. Wang S, Sun C, Li J, Zhang E, Ma Z, Xu W, Li H, Qiu M, Xu Y, Xia W, Xu L, Yin R. Roles of RNA methylation by means of N6-methyladenosine (m6A) in human cancers. Cancer Lett. 2017; 408:112–20. https://doi.org/10.1016/j.canlet.2017.08.030

16. S chöller E, Weichmann F, Treiber T, Ringle S, Treiber N, Flatley A, Feederle R, Bruckmann A, Meister G. Interactions, localization, and phosphorylation of the m6A generating METTL3-METTL14-WTAP complex. RNA. 2018; 24:499–512. https://doi.org/10.1261/rna.064063.117

17. Tang C, Klukovich R, Peng H, Wang Z, Yu T, Zhang Y, Zheng H, Klungland A, Yan W. ALKBH5-dependent m6A demethylation controls splicing and stability of long 3'-UTR mRNAs in male germ cells. Proc Natl Acad Sci USA. 2018; 115:E325–33. https://doi.org/10.1073/pnas.1717794115

18. Wojtas MN, Pandey RR, Mendel M, Homolka D, Sachidanandam R, Pillai RS. Regulation of m6A Transcripts by the 3'→5' RNA Helicase YTHDC2 is essential for a successful meiotic program in the mammalian germline. Mol Cell. 2017; 68:374–387.e12. https://doi.org/10.1016/j.molcel.2017.09.021

19. Ding C, Zou Q, Ding J, Ling M, Wang W, Li H, Huang B. Increased N6-methyladenosine causes infertility is associated with FTO expression. J Cell Physiol. 2018; 233:7055–66. https://doi.org/10.1002/jcp.26507

20. Wu R, Yao Y, Jiang Q, Cai M, Liu Q, Wang Y, Wang X. Epigallocatechin gallate targets FTO and inhibits adipogenesis in an mRNA m(6)A-YTHDF2-dependent manner. Int J Obes. 2018; 42:1378–88. https://doi.org/10.1038/s41366-018-0082-5

21. Kwok CT, Marshall AD, Rasko JE, Wong JJ. Genetic alterations of m6A regulators predict poorer survival in acute myeloid leukemia. J Hematol Oncol. 2017; 10:39. https://doi.org/10.1186/s13045-017-0410-6

22. Dai D, Wang H, Zhu L, Jin H, Wang X. N6-methyladenosine links RNA metabolism to cancer progression. Cell Death Dis. 2018; 9:124. https://doi.org/10.1038/s41419-017-0129-x

23. Wang CX, Cui GS, Liu X, Xu K, Wang M, Zhang XX, Jiang LY, Li A, Yang Y, Lai WY, Sun BF, Jiang GB, Wang HL, et al. METTL3-mediated m6A modification is required for cerebellar development. PLoS Biol. 2018; 16:e2004880. https://doi.org/10.1371/journal.pbio.2004880

24. Sánchez-Vásquez E, Alata Jimenez N, Vázquez NA, Strobl-Mazzulla PH. Emerging role of dynamic RNA modifications during animal development. Mech Dev. 2018; 154:24–32. https://doi.org/10.1016/j.mod.2018.04.002

25. Visvanathan A, Patil V, Arora A, Hegde AS, Arivazhagan A, Santosh V, Somasundaram K. Essential role of METTL3-mediated m6A modification in glioma stem-like cells maintenance and radioresistance. Oncogene. 2018; 37:522–33. https://doi.org/10.1038/onc.2017.351

26. Cui Q, Shi H, Ye P, Li L, Qu Q, Sun G, Sun G, Lu Z, Huang Y, Yang CG, Riggs AD, He C, Shi Y. m(6)A RNA methylation regulates the self-renewal and tumorigenesis of glioblastoma stem cells. Cell Reports. 2017; 18:2622–34. https://doi.org/10.1016/j.celrep.2017.02.059

27. Zhang C, Cheng W, Ren X, Wang Z, Liu X, Li G, Han S, Jiang T, Wu A. Tumor purity as an underlying key factor in glioma. Clin Cancer Res. 2017; 23:6279–91. https://doi.org/10.1158/1078-0432.CCR-16-2598

28. Su R, Dong L, Li C, Nachtergaele S, Wunderlich M, Qing Y, Deng X, Wang Y, Weng X, Hu C, Yu M, Skibbe J, Dai Q, et al. R-2HG Exhibits Anti-tumor Activity by Targeting FTO/m6A/MYC/CEBPA Signaling. Cell. 2018; 172:90–105.e23. https://doi.org/10.1016/j.cell.2017.11.031

29. Warda AS, Kretschmer J, Hackert P, Lenz C, Urlaub H, Höbartner C, Sloan KE, Bohnsack MT. Human METTL16 is a N6-methyladenosine (m6A) methyltransferase that targets pre-mRNAs and various non-coding RNAs. EMBO Rep. 2017; 18:2004–14. https://doi.org/10.15252/embr.201744940

30. Chai R, Zhang K, Wang K, Li G, Huang R, Zhao Z, Liu Y, Chen J. A novel gene signature based on five glioblastoma stem-like cell relevant genes predicts the survival of primary glioblastoma. J Cancer Res Clin Oncol. 2018; 144:439–47. https://doi.org/10.1007/s00432-017-2572-6

31. Jiang T, Mao Y, Ma W, Mao Q, You Y, Yang X, Jiang C, Kang C, Li X, Chen L, Qiu X, Wang W, Li W, et al, and Chinese Glioma Cooperative Group (CGCG). CGCG clinical practice guidelines for the management of adult diffuse gliomas. Cancer Lett. 2016; 375:263–73. https://doi.org/10.1016/j.canlet.2016.01.024

32. Chai RC, Zhang KN, Liu YQ, Wu F, Zhao Z, Wang KY, Jiang T, Wang YZ. Combinations of four or more CpGs methylation present equivalent predictive value for MGMT expression and temozolomide therapeutic prognosis in gliomas. CNS Neurosci Ther. 2019; 25:314–22. https://doi.org/10.1111/cns.13040

33. Yin AA, Lu N, Etcheverry A, Aubry M, Barnholtz-Sloan J, Zhang LH, Mosser J, Zhang W, Zhang X, Liu YH, He YL. A novel prognostic six-CpG signature in glioblastomas. CNS Neurosci Ther. 2018; 24:167–77. https://doi.org/10.1111/cns.12786

34. Chai RC, Liu YQ, Zhang KN, Wu F, Zhao Z, Wang KY, Jiang T, Wang YZ. A novel analytical model of MGMT methylation pyrosequencing offers improved predictive performance in patients with gliomas. Mod Pathol. 2019; 32:4–15. https://doi.org/10.1038/s41379-018-0143-2

35. Han B, Meng X, Chen H, Chen L, Liu X, Wang H, Liu D, Gao F, Lin L, Ming J, Sun B, Yin S, Wang R, et al. Epigenetic silencing of miR-338 facilitates glioblastoma progression by de-repressing the pyruvate kinase M2-β-catenin axis. Aging (Albany NY). 2017; 9:1885–97. https://doi.org/10.18632/aging.101271

36. Chen J, Sun Y, Xu X, Wang D, He J, Zhou H, Lu Y, Zeng J, Du F, Gong A, Xu M. YTH domain family 2 orchestrates epithelial-mesenchymal transition/proliferation dichotomy in pancreatic cancer cells. Cell Cycle. 2017; 16:2259–71. https://doi.org/10.1080/15384101.2017.1380125

37. Zhang S, Zhao BS, Zhou A, Lin K, Zheng S, Lu Z, Chen Y, Sulman EP, Xie K, Bögler O, Majumder S, He C, Huang S. m6A Demethylase ALKBH5 Maintains Tumorigenicity of Glioblastoma Stem-like Cells by Sustaining FOXM1 Expression and Cell Proliferation Program. Cancer Cell. 2017; 31:591–606.e6. https://doi.org/10.1016/j.ccell.2017.02.013

38. Wei J, Liu F, Lu Z, Fei Q, Ai Y, He PC, Shi H, Cui X, Su R, Klungland A, Jia G, Chen J, He C. Differential m6A, m6Am, and m1A Demethylation Mediated by FTO in the Cell Nucleus and Cytoplasm. Mol Cell. 2018; 71:973–985.e5. https://doi.org/10.1016/j.molcel.2018.08.011

39. Mauer J, Jaffrey SR Sr. FTO, m6 Am, and the hypothesis of reversible epitranscriptomic mRNA

modifications. FEBS Lett. 2018; 592:2012–22. https://doi.org/10.1002/1873-3468.13092

40. Deng X, Su R, Weng H, Huang H, Li Z, Chen J. RNA N6-methyladenosine modification in cancers: current status and perspectives. Cell Res. 2018; 28:507–17. https://doi.org/10.1038/s41422-018-0034-6

41. Xiang Y, Laurent B, Hsu CH, Nachtergaele S, Lu Z, Sheng W, Xu C, Chen H, Ouyang J, Wang S, Ling D, Hsu PH, Zou L, et al. RNA m6A methylation regulates the ultraviolet-induced DNA damage response. Nature. 2017; 543:573–76. https://doi.org/10.1038/nature21671

42. Li HB, Tong J, Zhu S, Batista PJ, Duffy EE, Zhao J, Bailis W, Cao G, Kroehling L, Chen Y, Wang G, Broughton JP, Chen YG, et al. m6A mRNA methylation controls T cell homeostasis by targeting the IL-7/STAT5/SOCS pathways. Nature. 2017; 548:338–42. https://doi.org/10.1038/nature23450

43. Bøvelstad HM, Nygård S, Størvold HL, Aldrin M, Borgan Ø, Frigessi A, Lingjaerde OC. Predicting survival from microarray data--a comparative study. Bioinformatics. 2007; 23:2080–87. https://doi.org/10.1093/bioinformatics/btm305

44. Sauerbrei W, Royston P, Binder H. Selection of important variables and determination of functional form for continuous predictors in multivariable model building. Stat Med. 2007; 26:5512–28. https://doi.org/10.1002/sim.3148

45. Hu X, Martinez-Ledesma E, Zheng S, Kim H, Barthel F, Jiang T, Hess KR, Verhaak RG. Multigene signature for predicting prognosis of patients with 1p19q co-deletion diffuse glioma. Neuro Oncol. 2017; 19:786–95. https://doi.org/10.1093/neuonc/now285

46. Zhou Z, Huang R, Chai R, Zhou X, Hu Z, Wang W, Chen B, Deng L, Liu Y, Wu F. Identification of an energy metabolism-related signature associated with clinical prognosis in diffuse glioma. Aging (Albany NY). 2018; 10:3185–209. https://doi.org/10.18632/aging.101625

Supplementary Figures
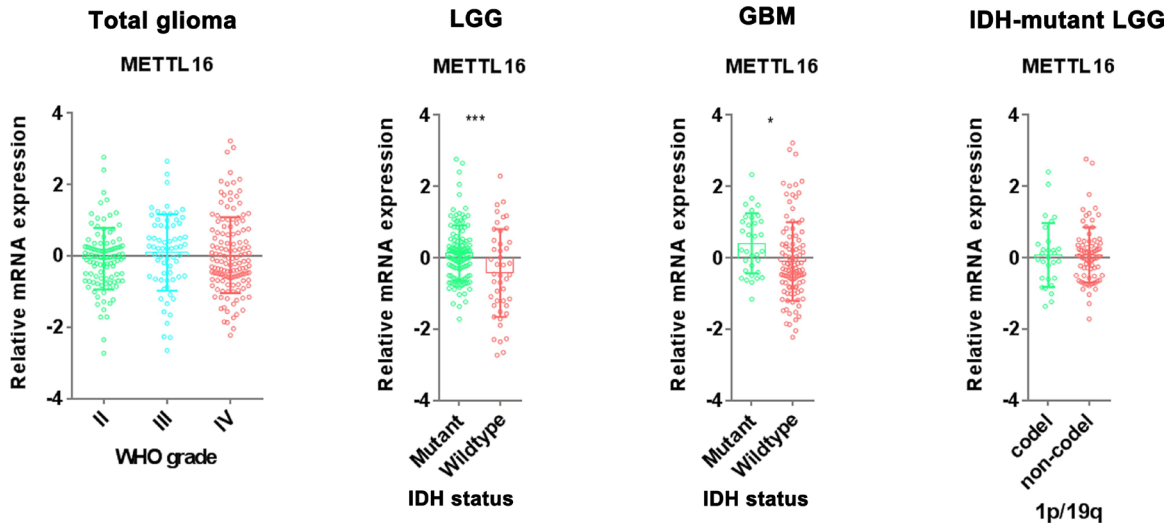
Figure S1. Expression of METTL16 in gliomas with different clinicopathological features.
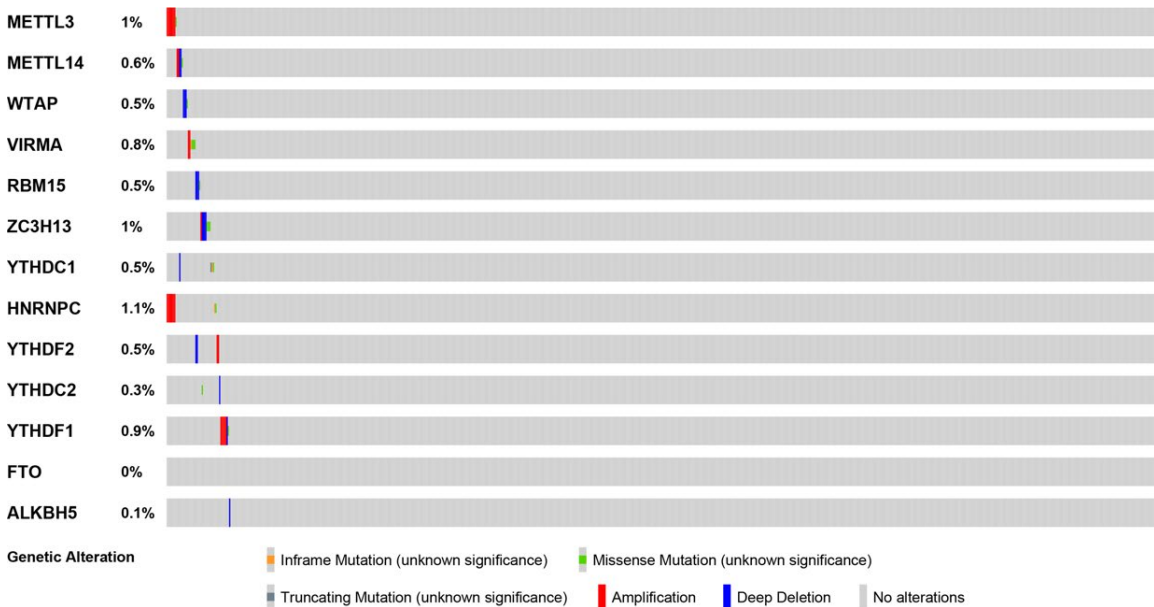
Figure S2. Genetic changes of RNA m^{6}A regulators in TCGA dataset. Genetic changes of the thirteen m^{6}A regulators in the 595 gliomas from the TCGA dataset.
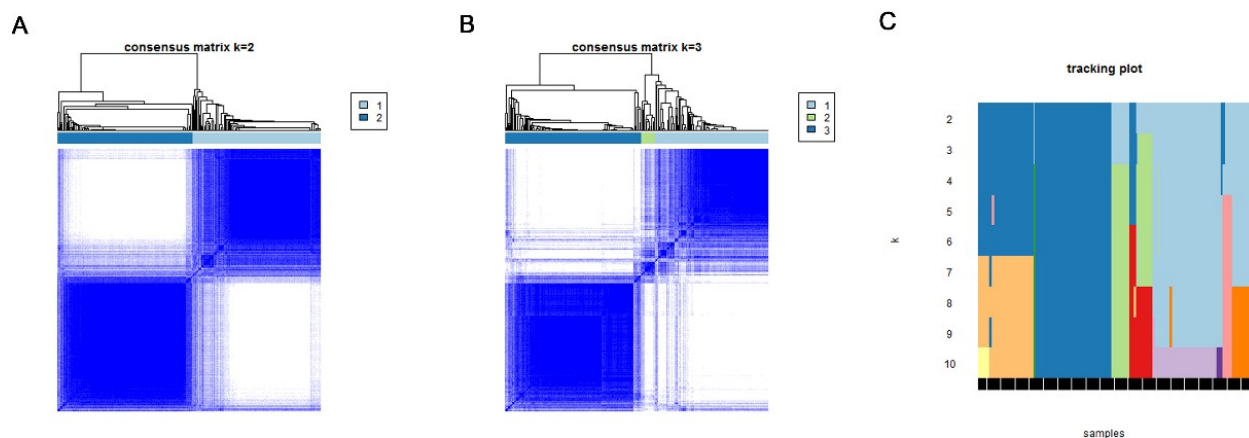
Figure S3. Identification of consensus clusters by m⁶A RNA methylation regulators. (**A-B**) Consensus clustering matrix for k = 2 (**A**) and k = 3 (**B**). (C) the tracking plot for k=2 to k=10.
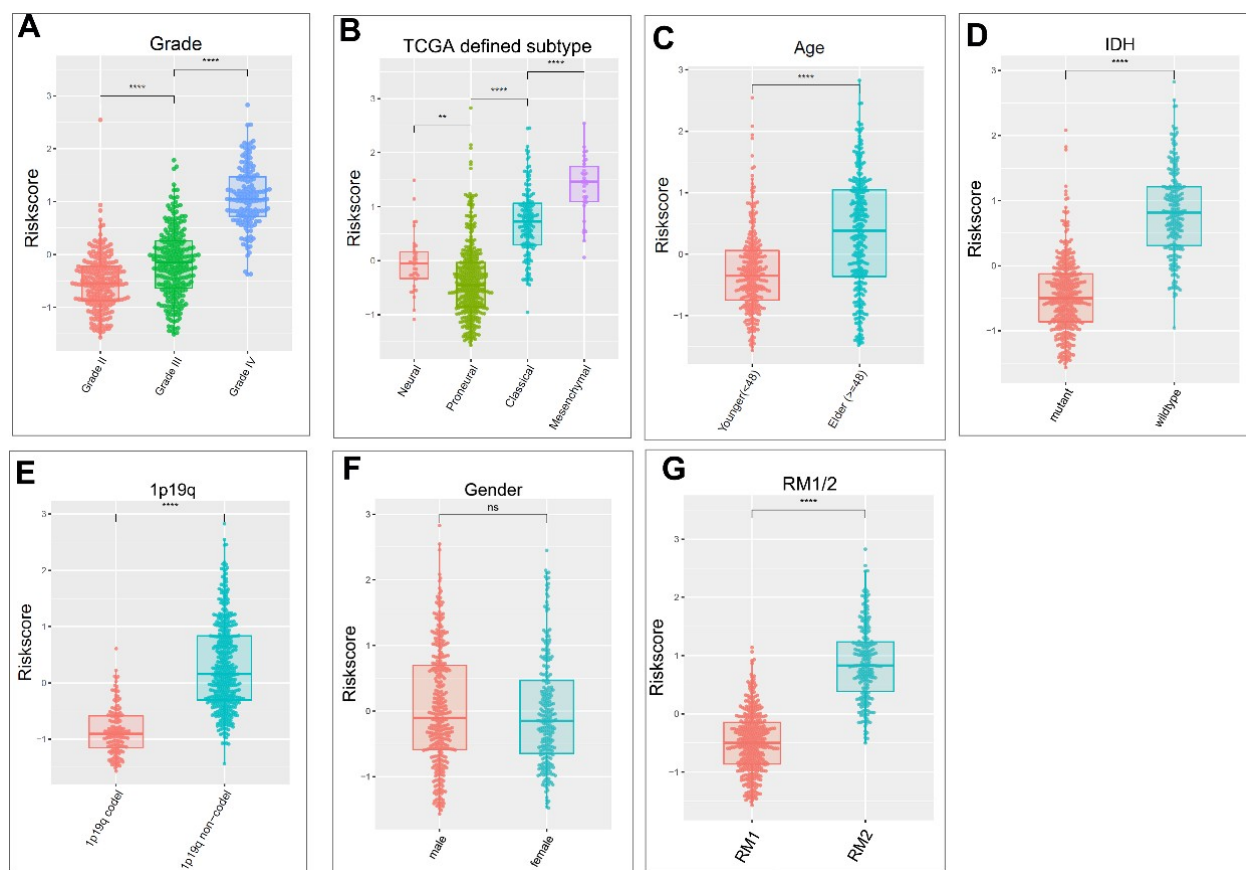
Figure S4. Relationship between the risk score, clinicopathological features and RM1/2 subgroups in the TCGA dataset. (**A–G**) Distribution of risk scores in the TCGA dataset stratified by WHO grade (A), TCGA subtype (B), age (C), *IDH* status (D), 1p/19q codel status (E), gender (F) and RM1/2 subgroups(G). ns no significance, ** P < 0.01, and **** P < 0.0001.
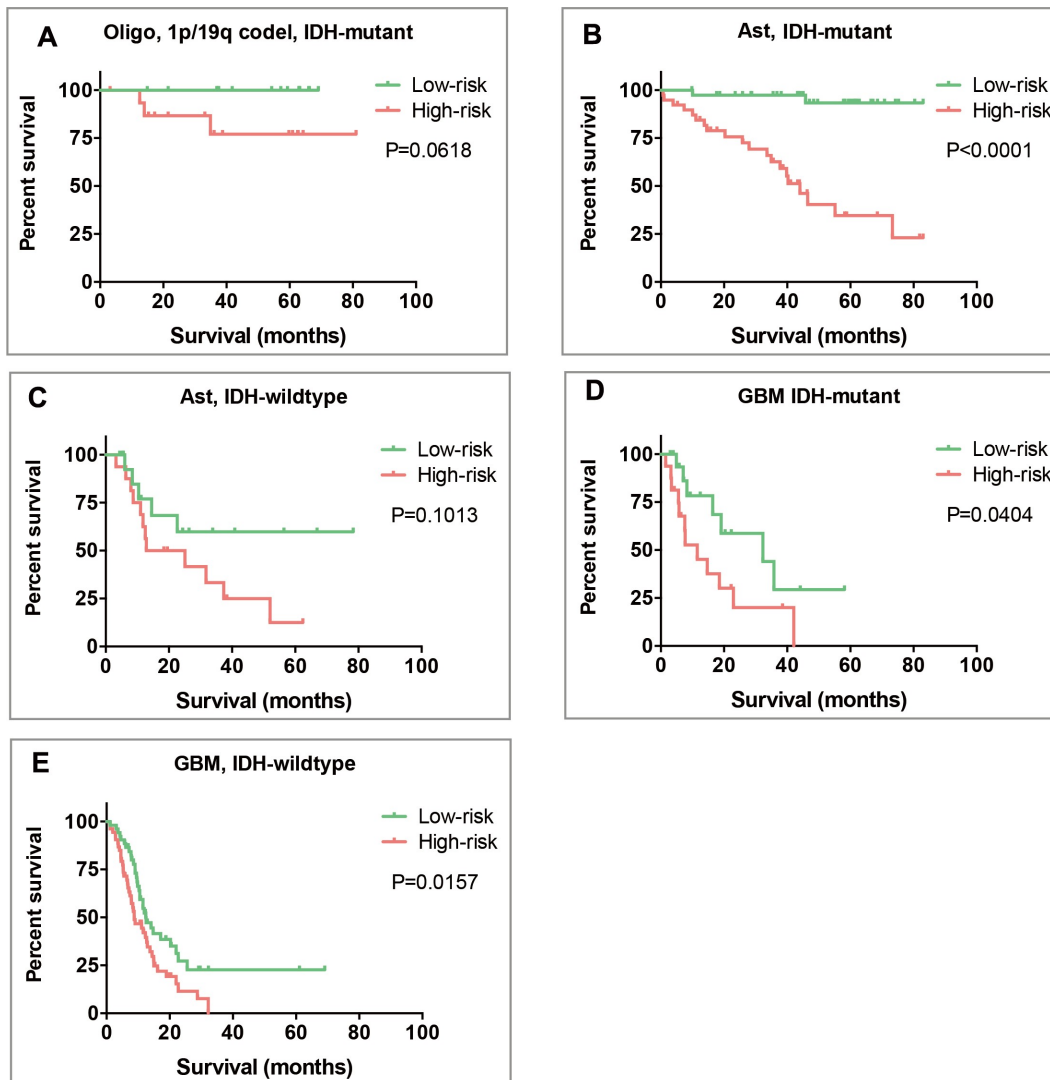
Figure S5. Prognostic value of the risk signature in patients stratified by the integrated analysis of WHO 2016.
(**A-E**) Kaplan–Meier overall survival curves for patients with Oligodendroglioma with IDH-mutant and 1p/19q co-deletion (**A**), Astrocytoma with IDH-mutant (**B**), Astrocytoma with IDH-wildtype (**C**), GBM with IDH-mutant (**D**), and GBM with IDH- wildtype (**E**).

Supplementary Tables

Table S1. Clinicopathological features of patients included in this study.

		CGGA dataset		TCGA dataset	
		Number	Percentage	Number	Percentage
Total		309	100.00%	595	100.00%
Age		8-81 (43)		14-89 (47)	
	< median	153	49.51%	292	49.08%
	≥ median	156	50.49%	303	50.92%
Gender					
	Female	115	37.22%	248	41.68%
	Male	194	62.78%	343	57.65%
Grade			0.00%		0.00%
	II	104	33.66%	211	35.46%
	III	67	21.68%	235	39.50%
	IV	138	44.66%	149	25.04%
IDH					
	Mutation	159	51.46%	373	62.69%
	Wildtype	150	48.54%	222	37.31%
1p19q					
	Codel	31	10.03%	148	24.87%
	Non-codel	220	71.20%	447	75.13%
	NA	58	18.77%	0	0.00%

Table S2. Clinicolpathological features are different between RM1 and RM2.

		RM1	RM2	P-value
Total cases		150	159	
Gender				6.739E-02
	Male	89	105	
	Female	61	54	
Age		40 (10-75)	46 (8-81)	2.460E-05
Grade				4.593E-150
	II	93	11	
	III	35	32	
	IV	22	116	
TCGA subtype				2.593E-108
	Neural	67	9	
	Proneural	67	32	
	Classical	13	56	
	Mesenchymal	3	62	
IDH				3.605E-60
	Mutant	122	37	
	Wildtype	28	122	
1p19q				1.137E-81
	Codel	29	2	
	Non-codel	96	124	
	NA	25	33	

Table S3. The prognosis value of m6A regulators in LGG.

m6A regulators	LGG				LGG, IDH-wildtype				LGG, IDH-mutant, 1p/19q noncodel				LGG, IDH-mutant, 1p/19q codel			
	HR	Confident Interval		P-value	HR	Confident Interval		P-value	HR	Confident Interval		P-value	HR	Confident Interval		P-value
		low	high			low	high			low	high			low	high	
YTHDF2	**2.76**	**2.08**	**3.66**	**1.79E-12**	**1.79**	**1.04**	**3.09**	**3.69E-02**	**6.78**	**3.25**	**14.12**	**3.24E-07**	18.65	0.56	625.01	1.03E-01
WTAP	**1.86**	**1.43**	**2.41**	**3.67E-06**	1.27	0.90	1.80	1.77E-01	**2.04**	**1.31**	**3.17**	**1.58E-03**	263.02	0.38	180022.12	9.44E-02
ALKBH5	**2.24**	**1.59**	**3.18**	**4.89E-06**	1.35	0.79	2.32	2.77E-01	**3.10**	**1.57**	**6.13**	**1.12E-03**	10.06	0.12	831.49	3.06E-01
RBM15	**1.86**	**1.38**	**2.49**	**4.06E-05**	1.23	0.75	2.02	4.02E-01	**2.21**	**1.34**	**3.65**	**1.85E-03**	1.89	0.27	13.44	5.24E-01
KIAA1429	**1.96**	**1.41**	**2.73**	**7.24E-05**	**1.85**	**1.10**	**3.11**	**2.11E-02**	**2.19**	**1.31**	**3.66**	**2.69E-03**	2.51	0.07	86.05	6.10E-01
HNRNPC	**2.05**	**1.43**	**2.95**	**9.67E-05**	**1.52**	**1.03**	**2.24**	**3.29E-02**	**3.78**	**1.79**	**7.98**	**5.02E-04**	6.23	0.13	295.15	3.53E-01
YTHDF1	**1.61**	**1.15**	**2.26**	**5.56E-03**	**1.79**	**1.04**	**3.09**	**3.69E-02**	**2.56**	**1.28**	**5.15**	**8.19E-03**	18.58	0.05	7576.31	3.41E-01
FTO	**0.64**	**0.47**	**0.88**	**5.92E-03**	0.98	0.61	1.59	9.38E-01	**0.28**	**0.10**	**0.75**	**1.15E-02**	0.06	0.00	8.77	2.68E-01
METTL14	1.28	0.94	1.75	1.20E-01	1.37	0.94	1.99	1.00E-01	1.27	0.77	2.11	3.47E-01	3.18	0.01	707.04	6.74E-01
ZC3H13	0.85	0.61	1.18	3.24E-01	1.15	0.71	1.88	5.65E-01	**0.60**	**0.39**	**0.94**	**2.47E-02**	0.57	0.00	91.98	8.27E-01
YTHDC2	1.05	0.78	1.43	7.36E-01	1.21	0.78	1.87	3.91E-01	0.86	0.52	1.42	5.57E-01	0.63	0.03	14.74	7.73E-01
METTL3	1.00	0.74	1.37	9.80E-01	1.11	0.78	1.58	5.70E-01	0.92	0.53	1.57	7.49E-01	6.50	0.13	322.61	3.47E-01
YTHDC1	1.00	0.73	1.38	9.86E-01	1.35	0.88	2.06	1.67E-01	1.17	0.65	2.11	6.09E-01	0.64	0.00	229.68	8.83E-01

Table S4. The prognosis value of m6A regulators in GBM.

m6A regulators	GBM				GBM, IDH-wildtype				GBM, IDH-mutant			
	HR	Confident Interval		P-value	HR	Confident Interval		P-value	HR	Confident Interval		P-value
		low	high			low	high			low	high	
	0.62	**0.47**	**0.81**	**5.56E-04**	**0.69**	**0.50**		**2.49E-02**	**0.38**	**0.15**	**0.96**	**4.06E-02**
	2.04	**1.23**	**3.37**	**5.79E-03**	**2.13**	**1.23**		**7.12E-03**	2.71	0.74	9.92	1.33E-01
KIAA1429	**1.71**	**1.15**	**2.53**	**7.64E-03**	1.58	1.00	2.52	5.20E-02	2.24	0.99	5.08	5.36E-02
METTL3	0.73	0.51	1.05	8.91E-02	0.74	0.47	1.16	1.90E-01	1.11	0.42	2.97	8.33E-01
ALKBH5	1.41	0.89	2.26	1.47E-01	1.60	0.95	2.69	7.47E-02	0.78	0.26	2.35	6.64E-01
RBM15	1.27	0.91	1.78	1.64E-01	**1.50**	**1.01**	**2.21**	**4.29E-02**	1.16	0.52	2.57	7.16E-01
ZC3H13	1.36	0.86	2.15	1.84E-01	1.13	0.60	2.11	7.06E-01	1.72	0.81	3.63	1.55E-01
YTHDC2	1.35	0.83	2.19	2.29E-01	1.43	0.82	2.49	2.08E-01	1.50	0.51	4.40	4.64E-01
WTAP	1.16	0.90	1.51	2.52E-01	1.03	0.78	1.37	8.12E-01	1.72	0.63	4.70	2.94E-01
HNRNPC	1.25	0.80	1.97	3.32E-01	1.16	0.70	1.90	5.66E-01	2.28	0.79	6.60	1.27E-01
YTHDC1	0.77	0.44	1.35	3.64E-01	1.00	0.49	2.05	9.98E-01	0.82	0.25	2.68	7.46E-01
METTL14	0.85	0.54	1.35	4.94E-01	0.90	0.55	1.46	6.57E-01	0.73	0.18	2.97	6.59E-01
YTHDF1	0.91	0.60	1.39	6.65E-01	0.87	0.56	1.35	5.31E-01	1.14	0.32	4.02	8.41E-01